https://doi.org/10.15255/KUI.2019.038
KUI-9/2020
Original scientific paper
Received August 25, 2019
Accepted December 12, 2019

Artificial Intelligence and Mathematical Modelling of the Drying Kinetics of Pharmaceutical Powders

S. Keskes,[a,b*] *S. Hanini*,[b] *M. Hentabli*,[a,b] and *M. Laidi*[b]

[a] Laboratory Quality Control, Physico-Chemical Department, SAIDAL of Médéa, Algeria
[b] Laboratory of Biomaterials and Transport Phenomena (LBMPT), Faculty of Technology, University Yahia Fares of Médéa, Algeria

Abstract

The study aims at modelling the drying kinetics of a pharmaceutical powder with active ingredient *Candesartan Cilexetil*. The kinetics was carried out in a vacuum dryer at different temperature levels, pressure, initial mass, and water content. The effect of some operating parameters on the drying time was studied. The modelling of drying times was based on the use of experimental design method. The data obtained were adjusted using 17 semi-empirical models, one proposed, a static ANN and DA_SVMR, regrouping all studied kinetics. The proposed model and DA_SVMR model were chosen as the most appropriate to describe the drying kinetics.

Keywords

Dragonfly algorithm, support vector machine regression (DA_SVMR), artificial neural network (ANN), mathematical modelling, drying kinetics, vacuum drying, Candesartan Cilexetil

1 Introduction

The drying engineering process plays an important role in improving the quality of the final product in many production processes, such as in the pharmaceutical industry. The drying process aims primarily at ensuring the conservation of certain pharmaceutical products, reducing their weight in order to facilitate carrying or solving certain issues, such as the caking of wet powders, and the contamination that causes corrosion due to the solvent or chemical degradation by slow hydrolysis.[1] The selection of a suitable dryer depends on the properties of the active ingredient, taking into consideration the heat-sensitivity of pharmaceutical powders. Numerous researchers have studied the drying time of various powders under different type of dryers, in order to investigate the influence of many operating conditions, such as vacuum pressure, temperature, dielectric loss factor, and moisture content.[2–4]

Due to several limitations, such as many hypotheses, complex and highly nonlinear behaviours, multivariable interaction, *etc.*, it is difficult to obtain an exact representative phenomenological model using conventional methods to fit and control the drying process. Thus, it is required to develop sophisticated methods to deal with all the above limitations.[5,6]

Several studies have shown growing interest in the application of artificial intelligence-based methods in modelling and control of non-linear behaviour drying process.[7] Moreover, a limited number of researchers have focused on the modelling of quality indicators of pharmaceutical powders by means of machine learning techniques (SVMR). SVMR modelling technique is known for its simplicity, optimisation adaptability, and handling the complex parameters.[8]

Several researchers have proposed mathematical models to describe the phenomenon of change in water content, heat transfer, and mass in drying. The equations can be theoretical, semi-theoretical, and empirical models.[9,33] The first of them only contains the internal resistance to mass transfer,[10] while others consider external resistance to mass transfer between product and air.[11] Theoretical models clearly explain the drying behaviour of the product and can be used in all process conditions, although they involve many hypotheses causing considerable errors.[12] The most used theoretical models are derived from diffusion. In the same way, semi-theoretical models are generally derived from Fick's second law and modifications of its simplified forms (other semi-theoretical models are derived from Newton's law of cooling). They are simpler and need fewer assumptions because of the use of some experimental results. On the other hand, they are only valid under the conditions of the applied process.[13] Empirical models have similar characteristics to semi-empirical models. They strongly depend on the experimental conditions and give limited information on the drying behaviour of the product.[11]

2 Experimental

The objective of this study was to experimentally determine the vacuum drying process time and modelling of drying kinetics of an active ingredient *Candesartan Cilexetil* under certain operating conditions. Furthermore, the obtained model of drying kinetics was investigated by different approaches.

* Corresponding author: Sonia Keskes, PhD
e-mail: soniakrispo@hotmail.com

Table 1 – Domain of studied factors

Variable category	Factors	Unit	Domain	STD	Variance	KURTOSIS
Input	temperature/T	°C	[40–60]	8.07	65.060	−1.4593
	pressure/p	bar	[0.4–0.8]	0	0.0274	−1.540
	initial moisture/M_0	%	[10–20]	4.03	16.265	−1.459
	initial mass/m_0	g	[0.5–1.5]	0.5	0.1621	−1.459
Output	time/t	min	[4 –42]	8.66	75.021	−0.205

2.1 Experimental procedure and design of the drying process

The experimental study was conducted in the Quality Control Laboratory SAIDAL of Médéa, and the modelling part was carried out in the Laboratory of Biomaterials and Phenomena of Transport at the University of Médéa. It was conducted in a vacuum dryer where the effect of four operating parameters, including temperature (T = 40–60 °C), pressure (p = 0.4–0.8 bar), initial mass (m_0 = 0.5–1.5 g), and initial water content (M = 10–20 %) on the drying time where evaluated and optimised by means of a response surface methodology (RSM) that is based on a full factorial central composite face-centred (CCF) design. In this approach, four factors with three levels (3^4) for each factor were considered, leading to 81 tests, plus 3 experiments for the reproducibility of the model. Table 1 shows the domain of these factors.

The output results (time) were fitted to a second-order polynomial equation (quadratic model), according to the model in Eq. (1).

$$y = a_0 + \sum a_i x_i + \sum a_{ij} x_i x_j + \ldots + \sum a_{ii} x_i^2 + a_{ij\ldots\ldots z} x_i x_j \ldots\ldots x_z \quad (1)$$

where y is the answer or the magnitude of interest. This is measured during the experiment and obtained with a given precision. x_i represents the level assigned to factor i by the experimenter to perform a test. This value is perfectly known. It is even supposed that this level is determined without error (classical assumption of regression). a_0, a_i, a_{ij}, a_{ii} are the coefficients of the mathematical model adopted *a priori*. They are not known, and must be calculated from the results of the experiments. The MODEL software was used to produce diagrams, experiments, and the model.

The thin layer drying process was carried out in a vacuum oven using an aluminium sheet of equal contact surface (54 mm × 56 mm). The thickness of the sample varied from 1 to 4 mm. The time intervals varied with temperature and pressure. The initial moisture was determined using Karl Fischer. Table 2 specifies the active ingredient used in this work.

Table 2 – Specification of the powder ready for pharmaceutical use (European Pharmacopoeia, 2017)

Chemical formula	$C_{33}H_{34}N_6O_6$
Molecular weight/g mol^{-1}	610.67
Diameter	≤ 6 μm
Water content (norm)	≥ 0.3 %
Melting point	157–160 °C

2.2 Mathematical modelling

The moisture ratio of the *Candesartan Cilexetil* samples during the thin layer vacuum drying experiments was obtained using the Eq. (2):

$$M_R = \frac{M_t - M_e}{M_0 - M_e} \quad (2)$$

where M_t, M_0, and M_e are moisture content at any time of the drying process, initial, and equilibrium moisture content, respectively. The equilibrium moisture content is relatively negligible compared to M_t and M_0.

Table 3 summarizes 17 models in the literature and the proposed model. The obtained drying curves were processed for drying rates to find the most suitable model among the eighteen different models. Mathematical model parameters were optimised using hybrid program (genetic-algorithm-nonlinear-curve-fitting). We were mostly interested in the application of genetic algorithms coupled with nonlinear fitting methods (hybrid program) to obtain model coefficients (Fig. 1). To determine the coefficients, MATLAB R2009a software was used.

Table 3 – Mathematical thin-layer models applied to moisture ratio values

N°	Model	Equation	Refs
1.	Newton	$M_R = \exp(-kt)$	14
2.	Page	$M_R = \exp(-kt^n)$	15
3.	Modified Page II	$M_R = \exp(-(kt)^n)$	16
4.	Henderson and Pabis	$M_R = a\exp(-kt^n)$	17
5.	Yagcioglu	$M_R = a\exp(-kt) + c$	18
6.	Two_term	$M_R = a\exp(-kt) + b\exp(-k_1 t)$	19
7.	Two_term exponential	$M_R = a\exp(-kt) + (1-a)\exp(-kat)$	19
8.	Wang and Singh	$M_R = 1 + at + bt^2$	21
9.	Diffusion approach	$M_R = a\exp(-kt) + (1-a)\exp(-kbt)$	21
10.	Verma *et al.*	$M_R = a\exp(-kt) + (1-a)\exp(-gt)$	23
11.	Modified Henderson and Pabis	$M_R = a\exp(-kt) + b\exp(-k_1 t) + c\exp(-nt)$	24
12.	Simplified Fick's diffusion	$M_R = a\exp(-k(t/L^2))$	24
13.	Modifide Page II	$M_R = \exp(-k(t/L^2)^n)$	26
14.	Midilli and Kucuk	$M_R = a\exp(-kt^n) + bt$	27
15.	Demir *et al.*	$M_R = a\exp(-kt^n) + b$	28
16.	Weibull	$M_R = \exp(-(t/a)^n)$	29
17.	Hii	$M_R = a\exp(-kt^n) + b\exp(-k_1 t^n)$	30
18.	**Proposed model**	$M_R = a\exp(-kt) + b\exp(-kt^{1/n}) + c$	**In this study**

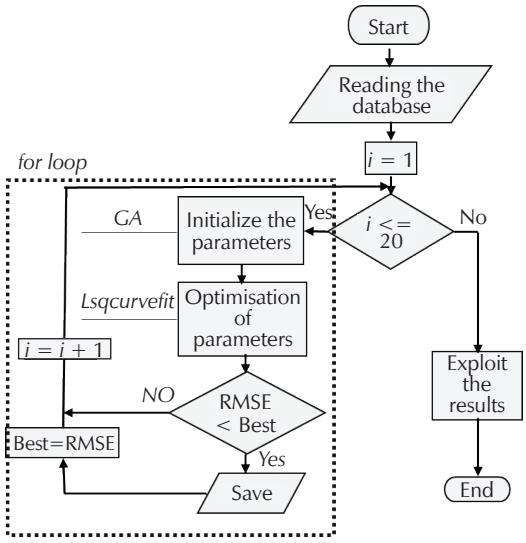

Fig. 1 – Hybrid program for determination of the model coefficients (genetic-algorithm-nonlinear-curve-fitting)

The best model was chosen using the analysis of statistical parameters, such as the coefficient of determination (R^2), the chi-square (χ^2), and square root of the mean square error (RMSE). These parameters were calculated by the form Eqs. (3–5).

$$R^2 = 1 - \frac{\sum_{i=1}^{N}(M_{R\,cal} - M_{R\,exp})^2}{\sum_{i=1}^{N}(M_{R\,exp} - \overline{M_{R\,exp}})^2} \quad (3)$$

$$\chi^2 = \frac{\sum_{i=1}^{n}(M_{R\,exp,i} - M_{R\,cal,i})^2}{N-n} \quad (4)$$

$$RMSE = \sqrt{\frac{1}{N}\sum_{i=1}^{N}\left(M_{R\,exp} - M_{R\,cal}\right)^2} \quad (5)$$

2.3 Artificial neural network

The idea of artificial neural networks was inspired by the way biological neurons proceed information. This concept

is utilised to carry out software simulations for the massively parallel processes, which involve processing elements that are interconnected in the network architecture. Learning in the human brain occurs in a network of neurons that are interconnected by axons, synapses, and dendrites. A variable synaptic resistance affects the run of information between two biological neurons. The artificial neuron receives inputs that are analogous to the electrochemical impulses that the dendrites of biological neurons receive from other neurons. Therefore, ANN can be considered a network of neurons, which are processing elements and weighted connections/weighing connections. The connections and weights are analogous to axons and synapses in the human brain, respectively. When simulating human brain analytical function, ANN has an intrinsic ability to learn and recognize highly non-linear and complex relationships by experience.[36] The procedure of weight adjustment is called back-propagation. A simplified procedure for the learning process of ANNs is summarised according to the following steps:

Step 1: Providing the network with training data consisting of input variables and target outputs.

Step 2: Evaluating the agreement of the network output with the target outputs.

Step 3: Adapting the connection weights between the neurons so the network produces better approximations of the desired target outputs.

Step 4: Continuing the process of adjusting the weights until some desired level of accuracy is achieved.

The modelling and simulation of a drying process goes by obtaining the data on how a drying process will behave without doing practical experiments.[37] The ANN implementation is composed of several stages that are thoroughly explained and summarised in the flow chart shown in Fig. 2.[38,39] All ANN calculations were conducted using free MATLAB R2009b software installed in Windows.

2.4 Support vector regression

Support vector machine regression (SVMR) analysis is a common machine learning tool for regression. It was first identified by *Vladimir Vapnik* and his colleagues in 1992.[40] SVM regression is considered a nonparametric technique because it relies on kernel functions (Table 4). This kernel function is included in MATLAB toolbox.

Table 4 – Kernel function

Kernel name	Kernel function
linear	$x^T z$
gaussian; RBF	$\exp\left(\frac{x-z}{2\sigma^2}\right)$
polynomial	$\left(1+x^T z\right)^p$ $p = 1,2,3\ldots.$

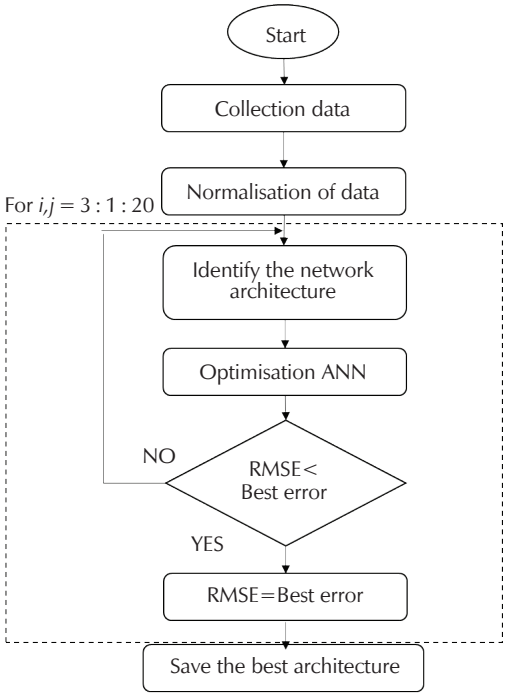

Fig. 2 – Flow chart of ANN training processes

The dual formula for nonlinear SVM regression replaces the inner product of the predictors ($x^T z$) with the corresponding element of the gram matrix nonlinear SVM regression to find the coefficients that minimize.[41]

$$L(\alpha) = \frac{1}{2}\sum_{i=1}^{N}\sum_{j=1}^{N}\left(\alpha_i - \alpha_i^*\right)\left(\alpha_j - \alpha_j^*\right)G\left(x_i, x_j\right) + \\ + \varepsilon\sum_{i=1}^{N}\left(\alpha_i - \alpha_i^*\right) - \sum_{i=1}^{N} y\left(\alpha_j - \alpha_j^*\right) \tag{6}$$

The function used to predict new values relies only on the media vectors:

$$f(x) = \sum_{n=1}^{N}\alpha_n - \alpha_{n^*})G\left(x_n, x\right) + b \tag{7}$$

The proposed model is based on SVMR learning algorithm, associated with DA algorithm for optimisation of its hyper-parameters. The division proportions of the data for training and test, along with the ranges of the hyper-parameters are the same as those for ANN. The steps leading to the development of the optimal DA-SVMR hybrid algorithm are illustrated in the flowchart presented in Fig. 3.

3 Results and discussion

3.1 Experimental design

The Table S1 (supplementary material) shows the experimental data for drying the powder. In this study, MODDE software (for Design of Experiments and Quality by Design analysis) was used to calculate the interaction effects and

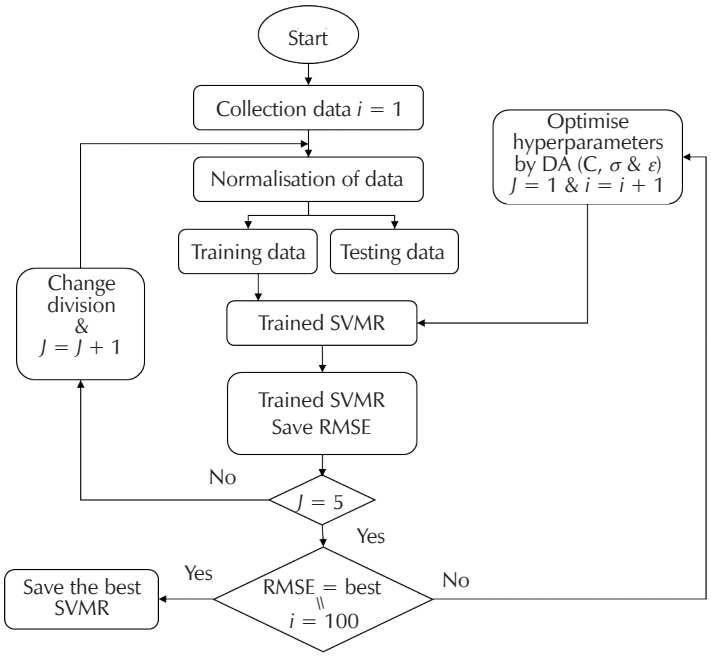

Fig. 3 – Flowchart of the proposed algorithm for trained (DA-SVMR)

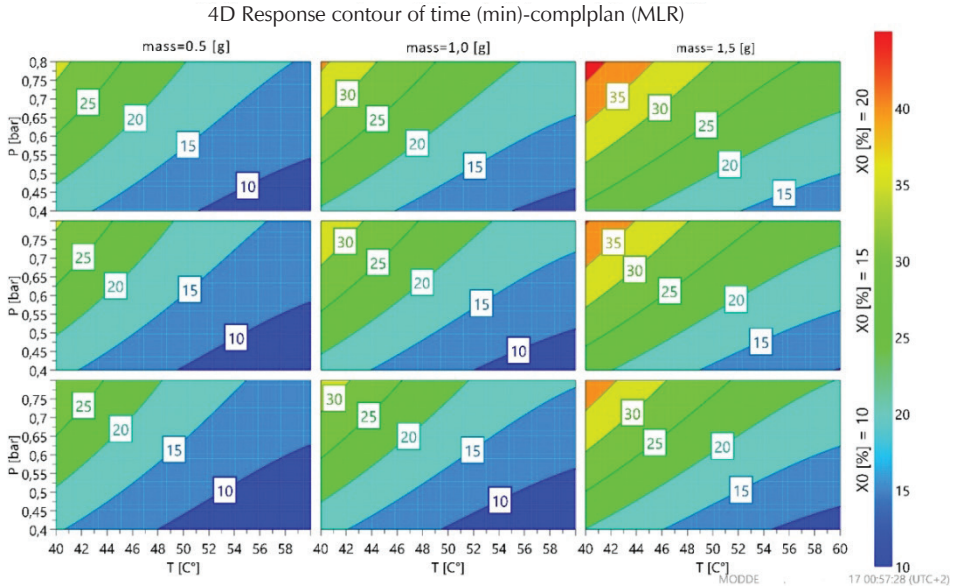

Fig. 4 – Iso-response curves of the modelling in drying time

the optimal parameter coefficients of the following second-order fitting model. In this model Eq. (12), a coefficient with a plus sign means that the factor has a synergetic effect on the drying time. According to this study, temperature is shown as the most influential parameter on drying process time. Interactions of statistical values $p < 0.05$ are neglected, and the model obtained by the experimental design was provided by the following form Eq. (8):

$$\begin{aligned} \text{Temps} = {} & 77.7645 - 11.6935m_0 + 0.2741M_0 + \\ & + 63.4722p - 2.9459T + 6.0319m_0^{\,2} + \\ & + 0.0273T^2 + 10.5556m_0p - 0.8472pT \end{aligned} \qquad (8)$$

The iso-response curves are graphical representations of all factors at all levels. The results of the interactions between four independent variables and the dependent variable are shown in Fig. 4. The software divided the zones according to the complete drying time in all the factors studied.

The results of the analysis of variance (ANOVA) summarised to test the validity of the model are presented in Table 5. The results were evaluated using descriptive statistical analysis, such as p-value, F-value, degree of freedom (d_f), and the coefficient of determination (R^2).

As shown in Table 6, a low probability value (p = 0.000) indicates that the model was highly significant. The high

Table 5 – Analysis of variance of model (ANOVA)

	Degree of freedom	Sum of squares	Mean squares	F-value	p-value	SD
model	8	6046.89	755.861	358.126	**0.000**	27.4929
residual	75	158.295	2.1106			1.45279
pure error	3	23.5675	7.85583			2.80283
total	84	36199.5	430.946			
	R^2_{adj} =	0.972	R^2 =	0.974		

value of the coefficient of determination (R^2 = 0.974) indicates a high reliability of the model.

3.2 Mathematical modelling of kinetics

For the mathematical modelling, the thin-layer drying equations, presented in Table 3, were tested to illustrate the drying curves of *Candesartan Cilexetil* (Figs. 5–7) under the nine experimental conditions. Among these experiments, nine kinetics at temperatures (60, 50, & 40 °C), mass (0.5, 1, and 1.5 g), initial water content 10 %, and pressure 0.8 bar (Figs. 5–7) were selected to apply the modelling and physical description.

Tables (S2–S4 & 6) report the results obtained when modelling the moisture content in thin-layer drying of this active ingredient and the optimised parameters of each model. A comparison between the semi-empirical models and proposed models in terms of RMSE show that the proposed model gives high performance when modelling the moisture content of the *Candesartan Cilexetil* samples throughout the thin-layer vacuum drying process. The proposed semi-empirical model was chosen as the most appropriate to describe the drying kinetics of the *Candesartan Cilexetil* powder. It has shown, respectively, a R^2 which varies from 0.999726 to 0.99999, and RMSE that varies between 0.077800 and $8.810405 \cdot 10^{-3}$ min for the nine-kinetics studied. The results of models 15 and 11 were close, but proposed model is preferable.

Fig. 8 represents evolution of the moisture ratio (*MR*) exp calculated by proposed model as a function of time at temperatures (40, 50, and 60 °C) and mass (0.5, 1, and 1.5 g).

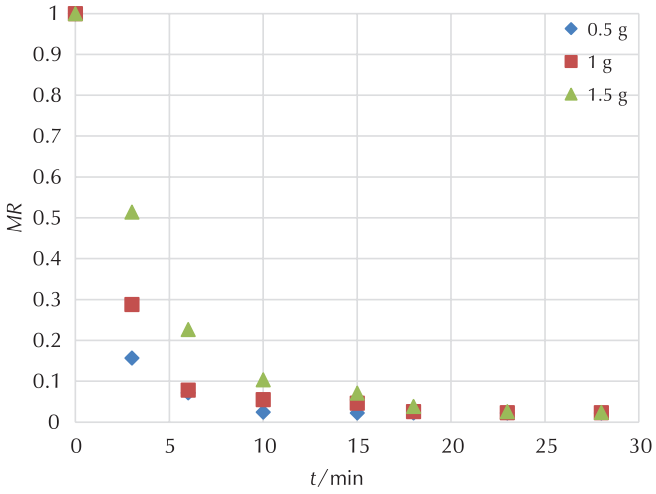

Fig. 6 – Evolution of the moisture ratio (*MR*) as a function of time at temperatures 50 °C, mass (0.5, 1, and 1.5 g), and initial water content 10 %

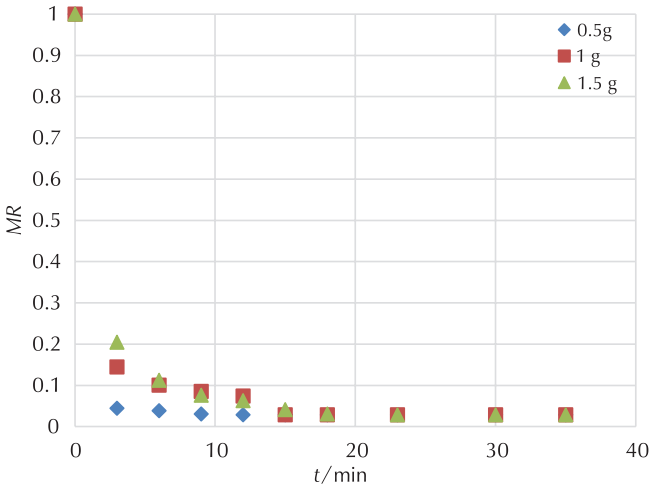

Fig. 5 – Evolution of the moisture ratio (*MR*) as a function of time at temperatures 60 °C, mass (0.5, 1, and 1.5 g), and initial water content 10 %

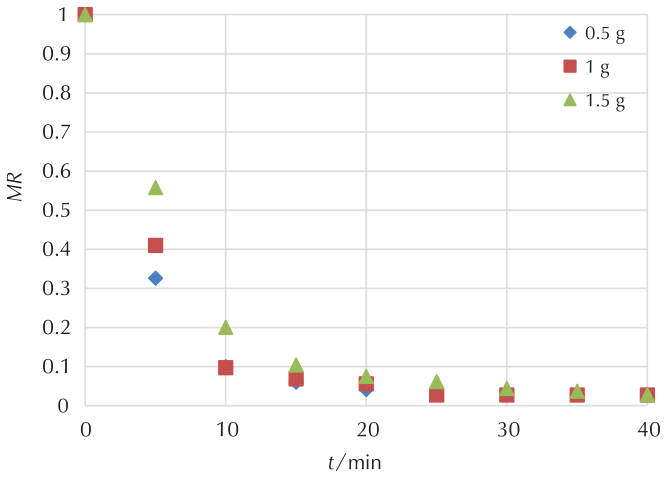

Fig. 7 – Evolution of the moisture ratio (*MR*) as a function of time at temperatures 40 °C, mass (0.5, 1, and 1.5 g), and initial water content 10 %

Table 6 – Performance comparison of the best selected models in terms of RMSE

Initial samples weight	T/°C	Model 11 · 10^3	Model 15 · 10^3	Proposed model · 10^3
0.5 g	60	2.27120	1.285600	0.158900
	50	7.94400	4.194000	0.077800
	40	11.6600	7.867000	1.193400
mean		7.29173	4.448870	0.476700
1 g	60	11.54027	10.27168	8.810405
	50	3.977283	07.11189	7.736377
	40	4.544892	08.85998	4.145978
mean		6.687483	8.747856	6.897587
1.5 g	60	8.091835	3.787095	3.755685
	50	5.340854	5.526422	5.339153
	40	1.891862	3.740056	1.284290
mean		5.108184	4.351191	3.459709
Global mean		**6.362466**	**5.849303**	**3.611332**

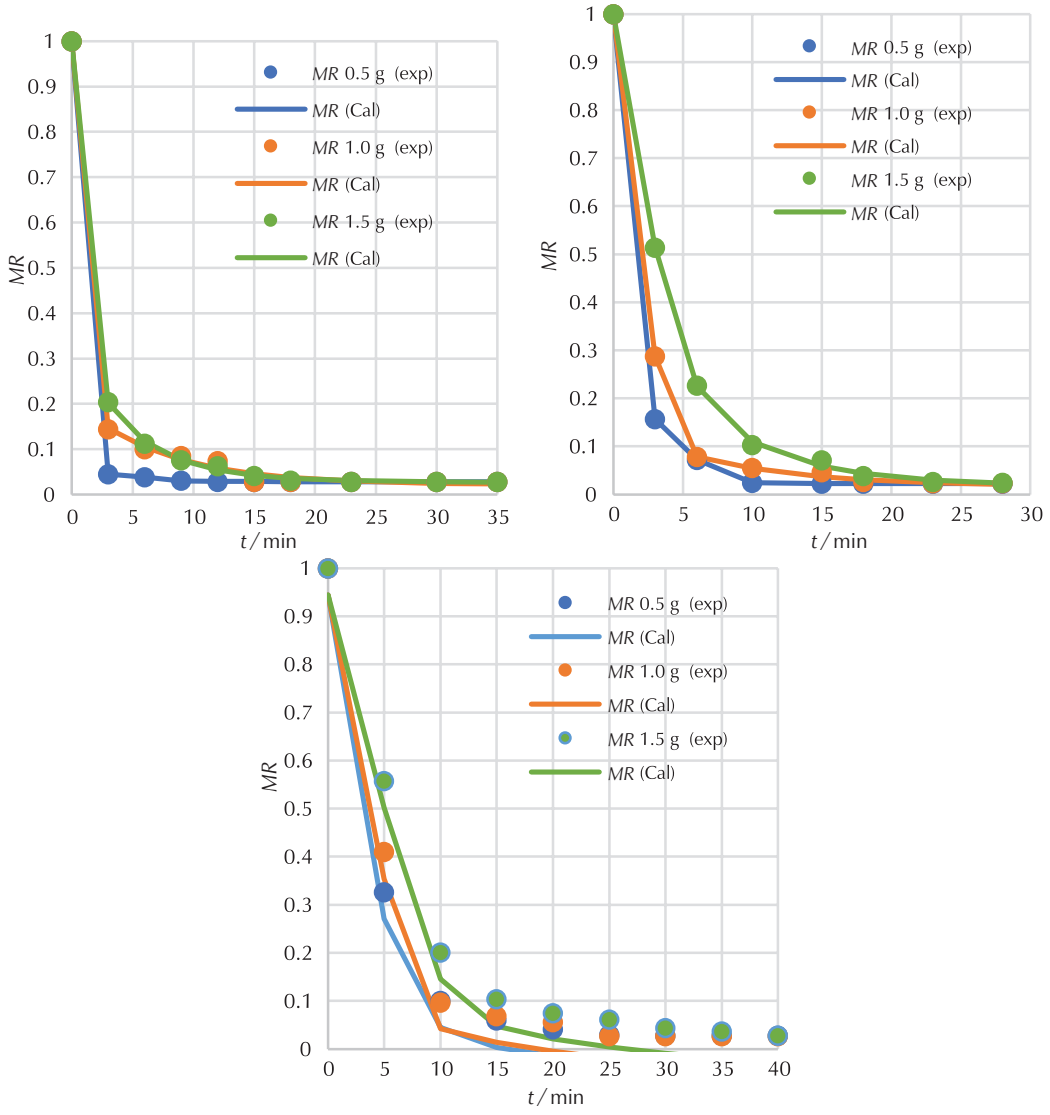

Fig. 8 – Evolution of the moisture ratio (*MR*) exp and cal by proposed model as a function of time at temperatures (40, 50, and 60 °C) and mass (0.5, 1, and 1.5 g)

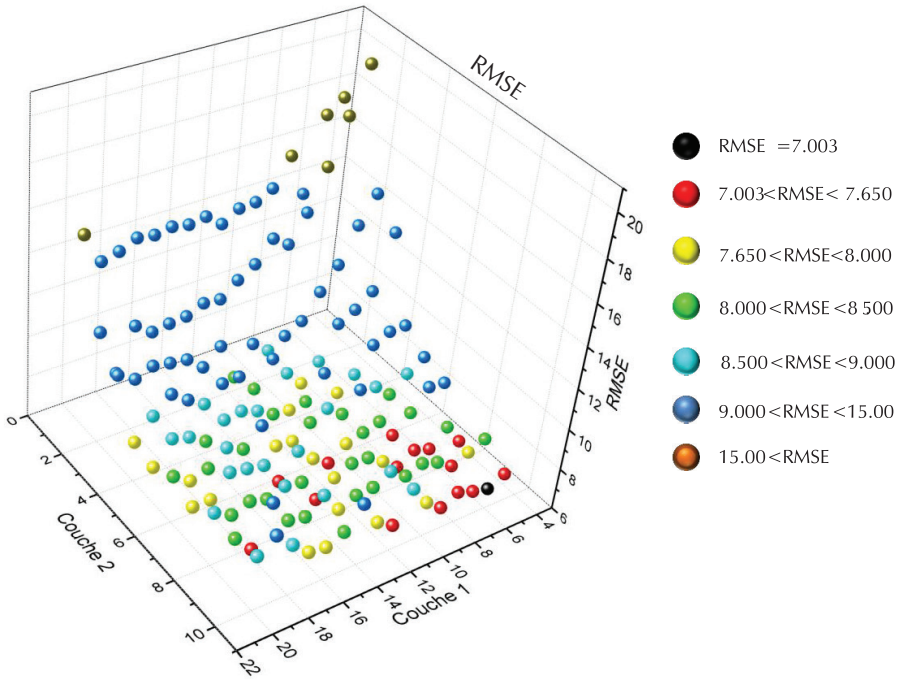

Fig. 9 – Results of neuronal variations in the hidden layers

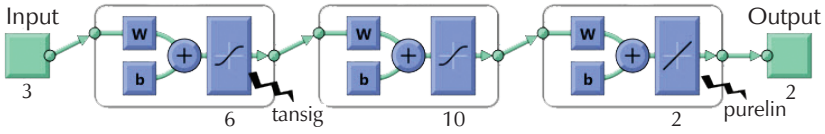

Fig. 10 – Multilayer neural networks for *MR* calculation

3.3 Artificial neural network modelling

There is no rule for choosing the number of neurons in the hidden layer.[38] In order to obtain the best neuronal structure, the number of neurons on the hidden layers has been optimised. In this study, we started with a hidden layer, varying the number of neurons hidden from 1 to 30, then an ANN with 2 hidden layers was tested where the number of neurons in the first layer ranged from 3 to 20 and the second layer from 1 to 10 neurons, each architecture was repeated 600 times to avoid convergence to the local minimum. Fig. 9 represents the error variation (RMSE) relative to the number of neurons in each hidden layer.

The result of optimisation of ANN, hidden layer 1 and 2 according to err (RMSE). Following the optimisation stage, an MLP with 6 neurons in the first hidden layer and 10 neurons in the second hidden layer, was quite acceptable for moisture content estimation based on the selected inputs mentioned earlier. Fig. 10 shows the architecture of optimised ANN.

To evaluate the predictive ability of a neural model, the latter must be tested for data that have been excluded from the learning base. Therefore, the linear regression of the ANN and the targeted (output) results of the ANN prediction were used. These are easily obtained using the *postreg* function of MATLAB®. Fig. 11 shows the linear re-

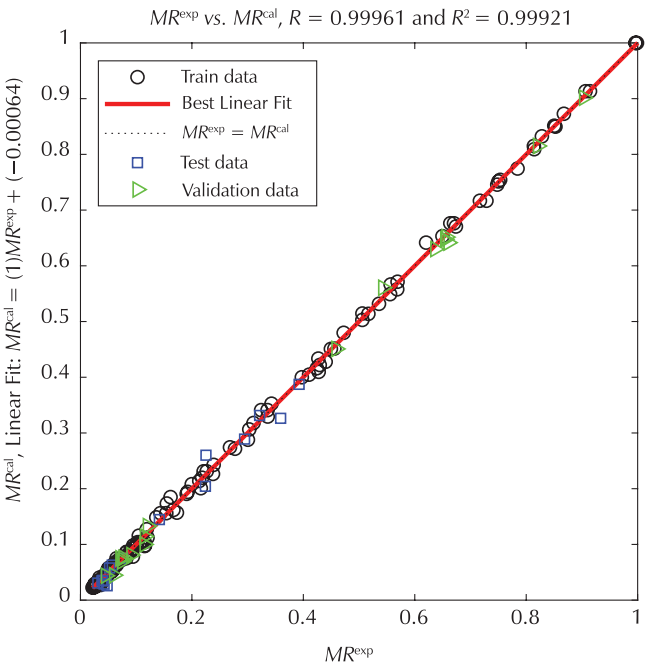

Fig. 11 – Linear *MR* regressions with MR^{exp} (All)

Table 7 – Parameters of the SVMR model

C	ε	γ	Kernel function	Quantity of support vectors	Cross-validation error	RMSE/–
40.5	0.0065	0.1576	Gaussian	75 %	$8.4 \cdot 10^{-4}$	0.0048

gression curve of the reduced water content *MR* calculated by ANN optimised with the experimental water content for all phases of learning, testing, and validation with a regression vector approaching the ideal [α (slope), β (intercept), *R* (correlation coefficient), R^2 (coefficient of determination) = [1, 0.00064, 0.99961]

3.4 Dragonfly algorithm support vector machine regression (DA-SVMR)

The optimisation of the SVMR model included the selection of the capacity parameter C, the ε-insensitive, loss function, and the corresponding parameters of the kernel function. Firstly, the kernel function should be decided. It defines the sample distribution in the mapping space. Usually, using the kernel function obtains better prediction performance,[42] and accordingly, it was used as the SVMR model kernel in this study. The kernel used is presented in Table 4, where γ is the parameter of the kernel, and *x* and *z* are two independent variables. Secondly, the corresponding parameters, *i.e.*, γ of the kernel function greatly affects the number of support vectors, which has a close relation with the performance of the SVMR and training time. Many support vectors could produce over-fitting and increase the training time. Additionally, γ controls the amplitude of the kernel function, and therefore, controls the generalisation ability of the SVMR. The ε-insensitive parameter prevents the entire training set from meeting the boundary conditions, and therefore allows the possibility of sparsity in the dual formulation's solution. The optimal value depends on the type of noise present in the data, which is usually unknown. Lastly, the effect of the capacity parameter C was tested. It controls the trade-off between maximising the margin and minimising the training error. If C is too low, then insufficient stress will be placed on fitting the training data. If C is much higher than the algorithm, it will overfit the training data. However, *Wang et al.*[43] indicated that prediction error was scarcely influenced by C. To make the learning process stable, a large value should be set up for C. Table 7 shows the best obtained parameters.

To optimise the SVMR model parameters, we used the algorithm mentioned in the experimental part. The SVMR model was trained and tested using a pre-processed data (X_{in}) on the basis of this proposed expression Eq. (9):

$$X_{in} = \sqrt[1/0.2]{X_i} \tag{9}$$

A scatter-plot of the observed against experimental data that are based on the SVMR results are depicted in Fig. 12. Results show a satisfactory performance with high determination coefficient of 0.99975 and very low RMSE of 0.0048.

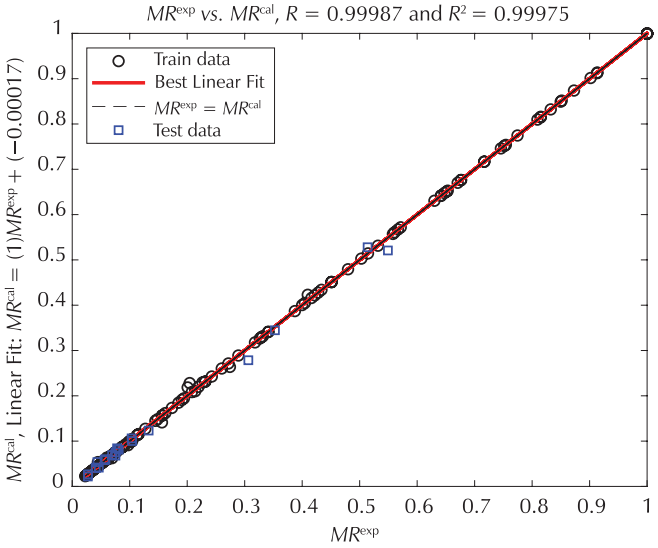

Fig. 12 – Experiment against observed drying time during training and test stage based on DA_SVMR result

3.5 Comparison between DA_SVMR and ANN models

The comparison of DASVMR and ANN models is based on the statistical parameters, learning time, and the complexity of the model. Table 8 presents the comparison of the modelling of SVMR and ANN according to the RMSE, *R*, R^2, number of parameters, and time.

Table 8 – Comparison between DA_SVMR and ANN models

Model	RMSE · 10^{-3}	*R*	R^2	Quantity to parameters
ANN	7.0	0.99961	0.99921	197
DA_SVMR	4.8	0.99987	0.99975	144

4 Conclusion

In light of the findings of this study, the following conclusions were drawn:

- The moisture content data of an active ingredient was experimentally determined throughout the process of vacuum drying under certain operating conditions.
- The obtained data were modelled by means of seventeen well-known semi-empirical models from literature, one semi-empirical model proposed in this work, and neural networks model.

- The results show that the proposed semi-empirical model demonstrated a higher performance to model the moisture content (*MR*) of the pharmaceutical powder of *Candesartan Cilexétil* in the drying process with higher determination coefficient ranging between {0.999726–0.99999} and very low RMSE ranging between $\{0.077800–8.810405) \cdot 10^{-3}$.
- In this work, the best model in terms of accuracy, smoothness, and flexibility is the hybrid model DA_SVMR.

ACKNOWLEDGEMENTS

Authors of this article gratefully acknowledge the employees of the SAIDAL of Médéa, Algeria and Laboratory of Biomaterials and Transport Phenomena (LBMPT), Faculty of Technology, University Yahia Fares of Médéa, Algeria, for their help and technical support during this work. Authors declare no conflict of interest.

List of symbols and abbreviations

a_0, a_i, a_{ij}, a_{ii}	– models parameters
ANN	– artificial neural network
C, ε-insensitive, γ	– *hyperplane parameters*
cal	– calculated
DA	– dragonfly algorithm
e	– thickness of the potato slices, mm
exp	– experimental
m	– initial mass, gram
M	– initial water content, %
MLP	– multi-layer perceptron
MR	– moisture ratio
P	– pressure, bar
R^2	– coefficient of determination
RMSE	– root mean squared error
RSM	– response surface methodology
SVMR	– support vector machine regression
t	– drying time, min
T	– temperature, °C
χ	– chi-square

References
Literatura

1. *A. Djebli, S. Hanini, O. Badaoui, M. Boumahdi*, A new approach to the thermodynamics study of drying tomatoes in mixed solar dryer, Sol. Energy **193** (2019) 164–174, doi: https://doi.org/10.1016/j.solener.2019.09.057.
2. *C. M. Mcloughlin, W. A. M. McMinn, T. R. A. Magee,* Microwave Drying of Pharmaceutical Powders, Food Bioprod. Process **78** (2000) 90–96, doi: https://doi.org/10.1205/096030800532798.
3. *C. M. McLoughlin, W. A. M. McMinn, T. R. A. Magee*, Microwave-Vacuum Drying of Pharmaceutical Powders, Dry Technol. **21** (2003) 1719–1733, doi: https://doi.org/10.1081/DRT-120025505.
4. *G. Farrel, W. A. M. McMinn, T. R. A. Magee*, Microwave-vacuum drying kinetics of pharmaceutical powders, Dry Technol. **23** (2005) 2131–2146, doi: https://doi.org/10.1080/07373930500212354.
5. *T. Ttayagarajan, M. Ponnavaikko, J. Shanmugam, R. C. Panda, P. G. Rao*, Artificial Neural Networks: Principle and Application To Model Based Control of Drying Systems – a Review, Dry Technol. **16** (1998) 931–966, doi: https://doi.org/10.1080/07373939808917449.
6. *M. Aghbashlo, S. Hosseinpour, A. S. Mujumdar*, Application of Artificial Neural Networks (ANNs) in Drying Technology: A Comprehensive Review, Dry Technol. **33** (2015) 1397–1462, doi: https://doi.org/10.1080/07373937.2015.1036288.
7. *V. Martínez-Martínez, J. Gomez-Gil, T. S. Stombaugh, M. D. Montross, J. M. Aguiar*, Moisture Content Prediction in the Switchgrass (*Panicum virgatum*) Drying Process Using Artificial Neural Networks, Dry Technol. **33** (2015) 1708–1719, doi: https://doi.org/10.1080/07373937.2015.1005228.
8. *E. A Zanaty*, Support Vector Machines (SVMs) *versus* Multilayer Perception (MLP) in data classification, Egypt Informatics J. **13** (2012) 177–183, doi: https://doi.org/10.1016/j.eij.2012.08.002.
9. *B. Ameri, S. Hanini, A. Benhamou, D. Chibane*, Comparative approach to the performance of direct and indirect solar drying of sludge from sewage plants, experimental and theoretical evaluation, Sol. Energy **159** (2018) 722–732, doi: https://doi.org/10.1016/j.solener.2017.11.032.
10. *M. Parti*, Selection of Mathematical Models for Drying Grain in Thin-Layers, J. Agric. Eng. Res. **54** (1993) 339–352, doi: https://doi.org/10.1006/jaer.1993.1026.
11. *M. Özdemir, Y. Onur Devres*, The thin layer drying characteristics of hazelnuts during roasting, J. Food Eng. **42** (1999) 225–233, doi: https://doi.org/10.1016/S0260-8774(99)00126-0.
12. *O. Badaoui, S. Hanini, A. Djebli, B. Haddad, A. Benhamou*, Experimental and modelling study of tomato pomace waste drying in a new solar greenhouse: Evaluation of new drying models, Renew. Energy **133** (2019) 144–155, doi: https://doi.org/10.1016/j.renene.2018.10.020.
13. *J. L. Parry,* Mathematical modelling and computer simulation of heat and mass transfer in agricultural grain drying: A review, J. Agric. Eng. Res. **32** (1985) (1985) 1–29, doi: https://doi.org/10.1016/0021-8634(85)90116-7.
14. *A. Mujumdar*, Handbook of Industrial Drying, New York and Basel, 1987.
15. *G. E. Page*, Factors Influencing the Maximum Rates of Air Drying Shelled Corn in Thin layers (1949).
16. *D. G. Overhults, G. M. White, H. E. Hamilton, I. J. Ross*, Drying soybeans with heated airn Trans ASAE **16** (1973) 112–113, doi: https://doi.org/10.13031/2013.37459.
17. *S. M. Hendorson, S. Pabis*, Grain Drying Theory (I) Temperature Effect on Drying Coefficient, J. Agric. Eng. Res. **6** (1961) 169–174.
18. *A. Yagcioglu, A. Degirmencioglu, F. Cagatay*, Drying characteristic of laurel leaves under different conditions, in: Proceedings of the 7th International Congress on Agricultural Mechanization and Energy, Faculty of Agriculture, Cukurova University, Adana, Turkey, 1999, pp. 565–569.
19. *S. M. Henderson*, Progress in developing the thin layer drying equation, Trans ASAE **17** (1974) 1167–1172, doi: https://doi.org/10.13031/2013.37052.

20. *D. Hutchinson, L. Otten*, Thin-layer air drying of soybeans and white beans. Int. J. Food Sci. Technol. **18** (2007) 507–522, doi: https://doi.org/10.1111/j.1365-2621.1983.tb00292.x.
21. *C. Y. Wang, R. P. Singh*, A single layer drying equation for rough rice, ASAE paper 8-3001, ASAE, St. Joseph, MI, 1978.
22. *A. S. Kassem*, Comparative studies on thin layer drying models for wheat, in: 13th international congress on agricultural engineering, 1998, pp. 2–6.
23. *L. R. Verma, R. A. Bucklin, J. B. Endan, F. T. Wratten*, Effects of drying air parameters on rice drying models, Trans. ASAE **28** (1985) 296–301, doi: https://doi.org/10.13031/2013.32245.
24. *V. T. Karathanos*, Determination of water content of dried fruits by drying kinetics, J. Food Eng. **39** (1999) 337–344, doi: https://doi.org/10.1016/S0260-8774(98)00132-0.
25. *L. M. Diamante, P. A. Munro*, Mathematical modelling of hot air drying of sweet potato slices, Int. J. Food Sci. Technol. **26** (1991) 99–109, doi: https://doi.org/10.1111/j.1365-2621.1991.tb01145.x.
26. *L. M. Diamante, P. A. Munro*, Mathematical modelling of the thin layer solar drying of sweet potato slices, Sol Energy **51** (1993) 271–276, doi: https://doi.org/10.1016/0038-092X(93)90122-5.
27. *A. Midilli, H. Kucuk, Z. Yapar*, A new model for single-layer drying, Dry Technol. **20** (2002) 1503–1513, doi: https://doi.org/10.1081/DRT-120005864.
28. *V. Demir, T. Gunhan, A. K. Yagcioglu*, Mathematical modelling of convection drying of green table olives, Biosyst. Eng. **98** (2007) 47–53, doi: https://doi.org/10.1016/j.biosystemseng.2007.06.011.
29. *O. Corzo, N. Bracho, A. Pereira, A. Vásquez*, Weibull distribution for modeling air drying of coroba slices, LWT – Food Sci. Technol. **41** (2008) 2023–2028, doi: https://doi.org/10.1016/j.lwt.2008.01.002.
30. *C. L. Hii, C. L. Law, M. Cloke*, Modeling using a new thin layer drying model and product quality of cocoa, J. Food. Eng. **90** (2009) 191–198, doi: https://doi.org/10.1016/j.jfoodeng.2008.06.022.
31. *J.-W. Bai, H.-W. Xiao, H.-L. Ma, C.-S. Zhou*, Artificial Neural Network Modeling of Drying Kinetics and Color Changes of Ginkgo Biloba Seeds during Microwave Drying Process, J. Food. Qual. **2018** (2018), doi: https://doi.org/10.1155/2018/3278595.
32. *J. Crank*, The mathematics of diffusion, Oxford University Press, 1979.
33. *A. Djebli, S. Hanini, O. Badaoui, B. Haddad, A. Benhamou*, Modeling and comparative analysis of solar drying behavior of potatoes, Renew. Energy **145** (2020) 1494–1506, doi: https://doi.org/10.1016/j.renene.2019.07.083.
34. *N. J. Thakor, S. Sokhansanj, F. W. Sosulski, S. Yannacopoulos*, Mass and dimensional changes of single canola kernels during drying, J. Food. Eng. **40** (1999) 153–160, doi: https://doi.org/10.1016/S0260-8774(99)00042-4.
35. *M. N. Ramesh, W. Wolf, D. Tevini, G. Jung*, Influence of processing parameters on the drying of spice paprika, J. FOod. Eng. **49** (2001) 63–72, doi: https://doi.org/10.1016/S0260-8774(00)00185-0.
36. *C. Si-Moussa, S. Hanini, R. Derriche, M. Bouhedda, A. Bouzidi*, Prediction of high-pressure vapor liquid equilibrium of six binary systems, carbon dioxide with six esters, using an artificial neural network model, Brazilian J. Chem. Eng. **25** (2008) 183–199, doi: https://doi.org/10.1590/S0104-66322008000100019.
37. *A. M. Ghaedi, A. Vafaei*, Applications of artificial neural networks for adsorption removal of dyes from aqueous solution: A review, Adv. Colloid Interface Sci. **245** (2017) 20–39 . doi: https://doi.org/10.1016/j.cis.2017.04.015.
38. *A. P. Plumb, R. C. Rowe, P. York, M. Brown*, Optimisation of the predictive ability of artificial neural network (ANN) models: A comparison of three ANN programs and four classes of training algorithm, Eur. J. Pharm. Sci. **25** (2005) 395–405, doi: https://doi.org/10.1016/j.ejps.2005.04.010.
39. *S. Haykin*, Neural Networks: A Comprehensive Foundation, 1st Ed. Prentice Hall PTR, Upper Saddle River, 1994, NJ, USA.
40. *V. Vapnik*, The nature of statistical learning theory, Springer Science & Business Media, 2000.
41. *T.-M. Huang, V. Kecman, I. Kopriva*, Kernel based algorithms for mining huge data sets, Springer, 2006.
42. *H.-T. Lin, C.-J. Lin*, A study on sigmoid kernels for SVM and the training of non-PSD kernels by SMO-type methods, Neural Comput. **3** (2003) 1–32.
43. *W. Wang, Z. Xu, W. Lu, X. Zhang,* Determination of the spread parameter in the Gaussian kernel for classification and regression, Neurocomp. **55** (2003) 643–663, doi: https://doi.org/10.1016/S0925-2312(02)00632-X.

SAŽETAK

Umjetna inteligencija i matematičko modeliranje kinetike sušenja farmaceutskog praha

Sonia Keskes,[a,b*] *Salah Hanini*,[a] *Mohamed Hentabli*[a,b] i *Mammar Laidi*[b]

Cilj rada je modeliranje kinetike sušenja farmaceutskog praha s aktivnim sastojkom *Candesartan Cilexetil*. Kinetika je izvedena u vakuumskoj sušilici pri različitim temperaturama, tlaku, početnoj masi i sadržaju vode. Proučavan je utjecaj nekih radnih parametara na vrijeme sušenja. Modeliranje vremena sušenja temeljilo se na primjeni eksperimentalne metode dizajna. Dobiveni podatci prilagođeni su pomoću 17 poluempirijskih modela, jednog predloženog, statičkog ANN i DA_SVMR, pregrupirajući svu proučavanu kinetiku. Predloženi model i model DA_SVMR pokazali su se kao najprikladniji za opisivanje kinetike sušenja.

Ključne riječi

Algoritam Dragonfly, regresija potpornih vektora (DA_SVMR), umjetna neuronska mreža (ANN), matematičko modeliranje, kinetika sušenja, vakuumsko sušenje, Candesartan Cilexetil

[a] *Laboratory Quality Control, Physico-Chemical Department, SAIDAL of Médéa, Alžir*

[b] *Laboratory of Biomaterials and Transport Phenomena (LBMPT), Faculty of Technology, University Yahia Fares of Médéa, Alžir*

Izvorni znanstveni rad

Prispjelo 25. kolovoza 2019.

Prihvaćeno 12. prosinca 2019.

Supplementary data

Table S1 – Experimental data

m/g	X_0/%	p/bar	T/°C	Time/min
0.5	10	0.4	40	15
1	10	0.4	40	16
1.5	10	0.4	40	21
0.5	15	0.4	40	16
1	15	0.4	40	17
1.5	15	0.4	40	22
0.5	20	0.4	40	17
1	20	0.4	40	20
1.5	20	0.4	40	24
0.5	10	0.6	40	24
1	10	0.6	40	26
1.5	10	0.6	40	30
0.5	15	0.6	40	24
1	15	0.6	40	27
1.5	15	0.6	40	30
0.5	20	0.6	40	25
1	20	0.6	40	28
1.5	20	0.6	40	34
0.5	10	0.8	40	30
1	10	0.8	40	35
1.5	10	0.8	40	38
0.5	15	0.8	40	32
1	15	0.8	40	35
1.5	15	0.8	40	40
0.5	20	0.8	40	30
1	20	0.8	40	35
1.5	20	0.8	40	42
0.5	10	0.4	50	10
1	10	0.4	50	10
1.5	10	0.4	50	12
0.5	15	0.4	50	10
1	15	0.4	50	12
1.5	15	0.4	50	15
0.5	20	0.4	50	12
1	20	0.4	50	12
1.5	20	0.4	50	15
0.5	10	0.6	50	13
1	10	0.6	50	15
1.5	10	0.6	50	19
0.5	15	0.6	50	15
1	15	0.6	50	17
1.5	15	0.6	50	22
0.5	20	0.6	50	14
1	20	0.6	50	17
1.5	20	0.6	50	25
0.5	10	0.8	50	18
1	10	0.8	50	21
1.5	10	0.8	50	27
0.5	15	0.8	50	19
1	15	0.8	50	23
1.5	15	0.8	50	28
0.5	20	0.8	50	22
1	20	0.8	50	25
1.5	20	0.8	50	30
0.5	10	0.4	60	4
1	10	0.4	60	6
1.5	10	0.4	60	7
0.5	15	0.4	60	6
1	15	0.4	60	7
1.5	15	0.4	60	9
0.5	20	0.4	60	7
1	20	0.4	60	9
1.5	20	0.4	60	12
0.5	10	0.6	60	10
1	10	0.6	60	12
1.5	10	0.6	60	15
0.5	15	0.6	60	10
1	15	0.6	60	13
1.5	15	0.6	60	16
0.5	20	0.6	60	11
1	20	0.6	60	15
1.5	20	0.6	60	18
0.5	10	0.8	60	13
1	10	0.8	60	14
1.5	10	0.8	60	20
0.5	15	0.8	60	14
1	15	0.8	60	16
1.5	15	0.8	60	22
0.5	20	0.8	60	15
1	20	0.8	60	17
1.5	20	0.8	60	24
1	15	0.6	50	11
1	15	0.6	50	11.5
1	15	0.6	50	11.8

Table S2 – Statistical analysis of models after optimisation for kinetics of mass 0.5 g

N°	T/°C	Parameters							Parameters' statistics			
		k	n	L	a	c	b	k_1	R^2	$X^2 \cdot 10^4$	RMSE · 10^3	χ^2Moy · 10^4
Mod1	60 50 40	1.00950 0.58525 0.21941							0.99201 0.99473 0.99508	7.90000 6.40000 6.60000	26.7715 23.6930 23.7770	6.96666
Mod2	60 50 40	2.96210 1.16277 0.32181	0.06009 0.44067 0.79820						0.99994 0.99902 0.99665	0. 06400 1.33000 5.19000	2.25900 9.99200 19.2480	2.19467
Mod3	60 50 40	343553 1.40770 0.24164	0.07050 0.44074 0.79821						0.99993 0.99902 0.99665	0.07200 1.33000 5.18700	2.40700 9.99100 19.2480	2.19633
Mod4	60 50 40	1.00944 0.58475 0.21898			0.99991 0.99858 0.99746				0.992013 0.994713 0.995070	8.95800 7.48200 7.90000	26.7710 23.6881 23.7579	8.11333
Mod5	60 50 40	1.39257 0.65172 0.24304			0.96995 0.97306 0.97029	0.03005 0.02643 0.03062			0.999907 0.999017 0.998739	0.11250 1.58400 2.39800	2.80570 9.95100 11.7050	1.36483
Mod6	60 50 40	0.01319 6.41236 0.01005			0.03919 0.70633 0.03897		0.96080 0.29347 0.96208	29.7562 0.21737 0.24654	0.999843 0.998210 0.998752	0.22100 3.69000 3.16500	3.63800 13.5820 11.6470	2.35866
Mod7	60 50 40	1.62293 1.17203 0.36834			0.48935 0.38176 0.43495				0.992159 0.995988 0.996594	8.79000 5.66000 5.35000	26.5124 20.6030 19.5510	6.60000
Mod8	60 50 40				-0.1108 -0.1307 -0.1042		0.00254 0.00364 0.00251		0.486520 0.662605 0.896880	943.130 693.300 190.400	274.683 228.040 116.620	608.943
Mod9	60 50 40	1.47787 0.04875 0.01129			0.96598 0.05916 0.03853		0.00459 14.7323 21.7276		0.999938 0.999374 0.998743	0.07370 1.01000 2.39000	2.27110 7.94400 11.6877	1.15790
Mod10	60 50 40	0.00678 0.04908 0.24631			0.03402 0.05943 0.96113		1.47723 0.71887 0.01000		0.999939 0.999374 0.998750	**0.07370** **1.01000** **2.38000**	**2.27120** **7.94400** **11.6600**	**1.15456**
Mod11	60 50 40	1.70000 0.76113 0.48475	1.69800 0.05219 0.05767		302.800 1.03881 2.45151	−301.79 0.06281 0.14451	0.03400 −0.1011 −1.5959	0.00600 10.4958 6.31183	0.999938 0.999335 0.999672	0.12980 2.68600 2.49000	2.27880 8.19400 5.96900	1.76860
Mod12	60 50 40	26.3579 52.8952 4.90130		5.10993 9.51087 4.73103	0.99991 0.99859 0.99746				0.978015 0.994712 0.995067	38.4700 8.97800 9.87800	49.0300 23.6880 23.7579	19.1087
Mod13	60 50 40	4.07829 7.52002 15.3607	0.06009 0.44106 0.79837	14.3089 −8.3049 11.2579					0.999940 0.999020 0.996650	0.07290 1.59700 6.48400	2.25900 9.99200 19.2480	2.71796
Mod14	60 50 40	2.74000 0.98277 0.23840	0.11871 0.58101 0.97951		0.99999 0.99999 1.00032		0.00039 0.00083 0.00115		0.999987 0.999878 0.998491	0.01770 0.24530 3.83000	1.03300 3.50262 12.8100	1.36433
Mod15	60 50 40	2.97398 0.95635 10.9206	0.26738 0.65197 −2.1013		0.97264 0.97998 0.97772		0.02736 0.01999 1.00002		0.999980 0.999825 0.999430	**0.02750** **0.35200** **1.44400**	**1.28560** **4.19400** **7.86700**	**0.60783**
Mod16	60 50 40				0.00000 0.71087 4.13854		0.07251 0.44091 0.79829		0.999928 0.999017 0.996646	0.07610 1.33100 5.18700	02.4679 9.99167 19.2480	2.19803
Mod17	60 50 40	18.5381 33.1056 14.3446	−66.470 −1.7241 −30.922		−3.0000 −2.9990 −3.0000		8.59710 14.5340 −21.132	−24.724 −25.313 −35.931	0.989727 0.963562 0.863038	18.6590 108.060 621.447	30.54491 63.65846 133.2502	249.389
Proposed model	60 50 40	1.54228 2.27393 0.11375	−0.2183 −0.1441 0.63649	30.3013 6250.99 0.01893	−29.301 −6249.9 0.21960	−30.273 −62509.7 0.76148			0.999999 0.999999 0.999986	**0.00050** **0.00016** **0.04984**	**0.15890** **0.07780** **1.19340**	**0.01683**

Table S3 – Statistical analysis of models after optimisation for kinetics of mass 1.0 g

N°	*T*/°C	Parameters							Parameters' statistics			
		k	n	L	a	c	b	k_1	R^2	$X^2 \cdot 10^4$	RMSE · 10^3	χ^2Moy · 10^4
Mod1	60 50 40	0.57420 0.40960 0.19040							0.9757935 0.9938633 0.9931500	24.089000 7.4651400 9.1061100	46.562750 25.557775 27.937855	13,5535
Mod2	60 50 40	1.38804 0.60358 0.16538	0.28728 0.70260 1.07338						0.9986904 0.9951707 0.9934320	1.3211926 6.6016495 10.639189	10.280827 22.251376 27.567047	6,18735
Mod3	60 50 40	3.13099 0.48840 0.18710	0.28728 0.70041 1.07036						0.9986905 0.9951688 0.9934280	1.3211926 6.6014938 10.639200	10.280827 22.251113 27.567072	6,18729
Mod4	60 50 40	0.57284 0.40921 0.19088			0.99660 0.99870 1.00310				0.9756502 0.9938498 0.9932042	27.086944 8.7064904 10.908389	46.550569 25.553606 27.913629	15,5673
Mod5	60 50 40	0.72530 0.45052 0.20382			0.95193 0.97065 0.98468	0.04742 0.03007 0.02097			0.9930065 0.998900 0.9945524	8.0194220 1.757170 10.571182	23.693027 10.479656 24.577786	6,78259
Mod6	60 50 40	0.07419 0.32485 0.22379			0.15499 0.74511 1.23319		0.84501 0.25481 −0.2332	1.23812 8.76288 55.6124	0.9984894 0.9942884 0.9940565	2.0414590 11.980690 16.208470	11.067409 24.475185 26.356178	10.0769
Mod7	60 50 40	1.10189 0.66397 0.24238			0.38117 0.44944 1.64200				0.9790939 0.9947597 0.9935664	23.215310 7.3438680 10.536810	43.095532 23.468917 27.434096	13.6987
Mod8	60 50 40				−0.1066 −0.1256 −0.1014		0.00239 0.00343 0.00240		0.5926412 0.7396349 0.9260606	713.28190 513.16500 134.39210	238.87769 196.18201 097.97669	453.613
Mod9	60 50 40	0.07417 0.02116 0.19627			0.15499 0.04457 0.99626		16.6897 21.9289 −0.3483		0.9984894 0.9990097 0.9947460	1.7498220 1.5786410 10.076900	11.067408 09.933030 23.996336	4.46845
Mod10	60 50 40	0.07419 0.02118 38.2547			0.15500 0.04458 −0.2284		1.23825 0.46411 0.22299		0.9984895 0.9990097 0.9940547	1.7498225 1.5786409 12.155539	11.067411 9.9330286 26.355308	5.16133
Mod11	60 50 40	0.08540 7.04544 9.25560	28.7820 1.10393 0.06130		0.1786 −4.6764 −7.7260	−2.9433 5.57460 0.16670	3.76470 0.10171 8.55910	2.76795 0.06104 0.67906	0.9983610 0.9998417 0.9998145	**3.3294477** **0.6327511** **1.4459233**	**11.540273** **3.9772828** **4.5448924**	**1.80271**
Mod12	60 50 40	21.6121 5.10324 10.7013		6.14331 3.53141 7.48749	0.99661 0.99900 1.00305				0.9756492 0.9938499 0.9932042	30.956500 10.447787 13.635487	46.550566 25.553606 27.913629	18.3465
Mod13	60 50 40	10.6222 31.5809 19.5385	0.28728 0.69923 1.07052	34.5316 16.8878 −9.2660					0.9986905 0.9951677 0.9934282	1.5099343 7.9219097 13.298900	10.280827 22.251278 27.567038	7.57691
Mod14	60 50 40	1.37930 0.46620 0.11080	0.29210 0.91790 1.31630		0.9999 1.0003 1.0006		4.9e-05 0.00120 0.00150		0.9986923 0.9980212 0.9974192	1.7586778 3.9730422 6.7423556	10.272325 14.094400 16.998768	4.15803
Mod15	60 50 40	1.38973 4.07950 34.0290	0.27807 −2.3422 −2.6286		1.00352 −0.9732 −0.9695		−0.0035 1.00002 1.00004		0.9986930 0.9994937 0.9992954	**1.758458** **1.011582** **1.831652**	**10.271684** **07.111898** **08.859987**	**1.53389**
Mod16	60 50 40				0.31939 2.05081 5.34697		0.28728 0.70220 1.07345		0.9986905 0.9951704 0.9934321	1.3211926 6.6015899 10.639202	10.280827 22.251275 27.567063	6.18732
Mod17	60 50 40	37.5710 6.27910 55.3890	−24.848 7.13831 5.83590		−2.9999 −3.0000 −3.0000		44.1689 5.68002 35.9444	−59.683 −2.6171 11.7388	0.9484470 0.8948138 0.7980636	95.89114 319.5577 933.3840	069.24274 109.46878 163.30379	449.611
Proposed model	60 50 40	0.13528 2.26934 0.03280	0.0999 −0.3611 0.46227	0.02158 2.56788 −0.0495	0.18695 −1.5682 0.19397	0.79141 −2.5370 0.85555			0.9990387 0.9994023 0.9998458	**1.5524646** **1.5960408** **0.6016198**	**8.8104048** **7.7363771** **4.1459784**	**1.25004**

Table S4 – Statistical analysis of models after optimisation for kinetics of mass 1.5 g

N°	T/°C	Parameters							Parameters' statistics			
		k	n	L	a	c	b	k_1	R^2	$X^2 \cdot 10^4$	RMSE $\cdot 10^3$	χ^2Moy $\cdot 10^4$
Mod1	60 50 40	0.46845 0.22781 0.13612							0.9813946 0.9957000 0.9894636	18.538795 5.3597061 11.743705	40.8471739 21.6558140 32.3092078	11.8807
Mod2	60 50 40	1.04669 0.25528 0.10860	0.39700 0.930061.10446						0.9993345 0.9960066 0.9905198	0.6758412 5.6785650 12.485455	07.3530469 20.6371600 31.1623327	6.27995
Mod3	60 50 40	1.12183 0.23036 0.13397	0.39703 0.92995 1.10449						0.9993345 0.9960064 0.9905199	0.6758412 5.6785688 12.485454	07.3530469 20.6371670 31.1623312	6.27996
Mod4	60 50 40	0.46625 0.22762 0.13733			0.99417 0.99917 1.01018				0.9812247 0.9956939 0.9897934	20.814043 6.2517927 13.263556	40.8059244 21.6537399 32.1186843	13.4431
Mod5	60 50 40	0.56329 0.24649 0.14769			0.95400 0.97800 0.99160	0.04432 0.02649 0.02353			0.9957362 0.9982553 0.9915638	4.9064327 2.8990586 12.296491	18.5324118 13.4607266 28.6315573	6.70066
Mod6	60 50 40	10.8551 0.22418 0.14244				0.72040 0.98370 1.01000	0.27960 0.01610 0.00420	0.12810 6.06950 −0.0530	0.9975516 0.9957006 0.9920060	3.3617210 9.3405126 13.961182	14.2022272 21.6107757 27.8499769	8.88781
Mod7	60 50 40	0.97947 0.32543 0.18308			0.35323 0.50489 1.72034				0.9858449 0.9966917 0.9909437	15.677124 04.674416 12.159485	35.4142612 18.7238137 30.7528486	10.8370
Mod8	60 50 40				−0.1059 −0.1128 −0.0758		0.00237 0.00292 0.00135		0.6357407 0.8912357 0.9228045	631.9006 196.9385 116.2001	224.83783 121.53349 095.06727	315.013
Mod9	60 50 40	0.06627 0.24661 0.14065			0.13790 0.97020 0.99610		11.1872 0.02354 −0.3788		0.9992025 0.9982166 0.9915330	0.9244435 2.9376166 11.988655	08.0443175 13.5499459 28.2708975	5.28357
Mod10	60 50 40	0.74089 0.24642 8.89885			0.86228 0.97068 −0.2329		0.06615 0.00497 0.16338		0.9992026 0.9982167 0.9923170	0.9.24450 2.9375557 12.004392	08.0443478 13.5498057 28.2894465	5.28880
Mod11	60 50 40	0.06710 10.3220 0.04400	0.76000 0.39900 8.27400		0.13960 −0.3992 0.17050	0.89700 1.21200 −1.1500	−0.0366 0.18702 1.97990	7.74190 0.07920 0.30952	0.9991935 0.9997255 0.9999635	**1.6369448** **1.1409889** **0.1073742**	**8.09183484** **5.34085378** **1.89186188**	**0.96177**
Mod12	60 50 40	29.2536 39.3837 18.2750		07.9210 13.1540 11.5360	0.99416 0.99917 1.01018				0.9812245 0.9956939 0.9897934	23.787478 7.5021512 15.474148	40.8059245 21.6537398 32.1186843	15.5879
Mod13	60 50 40	16.6379 13.7452 17.0476	0.39700 0.93030 1.10460	32.5698 8.52112 9.86304					0.9993345 0.9960069 0.9905201	0.7723900 6.8142844 14.566360	7.35304693 20.6371697 31.1623277	7.38435
Mod14	60 50 40	0.96127 0.22315 0.07694	0.46234 1.03635 1.29870		0.99999 1.00154 1.00249		0.00058 0.00122 0.00127		0.9998629 0.9981711 0.9966723	0.1846843 3.8155463 5.9000675	3.32882221 13.8122162 18.1047377	3.30010
Mod15	60 50 40	0.96590 3.72424 18.4958	0.50234 −1.4873 −1.9563		0.97810 −1.0050 −0.9791		0.02190 0.99990 1.00010		0.9998227 0.9997064 0.9998572	**0.2390348** **0.6108268** **0.2517842**	**3.78709460** **5.52642221** **3.74005528**	**0.36722**
Mod16	60 50 40				0.89139 4.34098 7.46416		0.39703 0.93036 1.10490		0.9993345 0.9960070 0.9905210	0.6758412 5.6785736 12.485453	07.3530469 20.6371756 31.1623299	6.27996
Mod17	60 50 40	21.162 14.384 3.1304	16.6610 −20.030 −16.240		−3.0000 −3.0000 −3.0000		31.6190 −0.4020 −23.870	−17.492 −2.5160 29.0168	0.9262146 0.6664565 0.6334615	0038.3632 1112.6545 0939.6110	083.175480 204.265800 204.353830	696.876
Proposed model	60 50 40	0.20559 0.15549 0.04200	−0.8131 0.63293 0.57492	0.73959 0.01756 −0.0090	0.26039 0.42539 0.19635	−0.7145 0.55674 0.81270			0.9998256 0.9997259 0.9999832	**0.2821034** **0.7601747** **0.0371114**	**3.75568484** **5.33915274** **1.28428953**	**0.35980**